DOI: 10.1002/ejic.200800267

Synthesis, Structure and Spectroscopic Properties of Lanthanide Complexes of *N*-Confused Porphyrins

Xun-Jin Zhu,[a] Feng-Lei Jiang,[a] Chun-Ting Poon,[a] Wai-Kwok Wong,*[a] and Wai-Yeung Wong[a]

Keywords: N ligands / Lanthanides / Porphyrinoids / Agostic interactions / Fluorescence

A series of *meso*-substituted *N*-confused porphyrins (NCP) is synthesized using the modified Rothemund–Lindsey procedure. Lanthanide *N*-confused porphyrinate complexes of the general formula [(NCP)Ln(L_{OMe})] [Ln^{3+} = Yb^{3+} and Er^{3+}; L_{OMe^-} = (η^5-C_5H_5)Co{P(=O)(OMe)$_2$}$_3^-$] are obtained in moderate yields upon interaction of *N*-confused porphyrin free bases (H_2NCP) with Ln[N(SiMe$_2$)$_3$]·x[LiCl(THF)$_3$], followed by the addition of the tripodal anion L_{OMe^-} as an effective encapsulating agent for the lanthanide ions. The structural and spectroscopic data for these complexes provide evidence for an η^2-agostic interaction between the Ln^{3+} ion and the inner C–H bond of the NCP ligand. Methylation of [(NCTCPP)Yb(L_{OMe})] (H_2NCTCPP = 2-azo-5,10,15,20-tetracyanophenyl-21-carbaporphyrin) with methyl iodide yields the novel stable lanthanide complex of the *N*-methylated derivative of *N*-confused porphyrins, whose X-ray structure also exhibits an η^2-agostic interaction between the metal center and the inner C–H bond of the NCTCPP ligand. The photophysical properties of the *N*-confused porphyrins and their lanthanide complexes are investigated.

Introduction

Porphyrin is a widely studied functional pigment that can coordinate to a variety of metals with four pyrrolic nitrogen atoms in a square-planar arrangement in the coordination core. In 1994, Latos-Grażyński and Furuta independently isolated a completely different isomer of porphyrin, namely an *N*-confused porphyrin (NCP), from the reaction between pyrrole and aryl aldehyde in a condensation protocol,[1–4] in which one of the pyrrole rings is connected to the *meso*-carbon atoms at the α and β positions. This isomer, formally classified as an *N*-confused porphyrin or carbaporphyrin, shows characteristic properties due to the confused pyrrole ring, which possesses an inner core carbon and a peripheral nitrogen in the skeleton. Since then Lindsey et al. have improved the synthetic method greatly[5] and Furuta has further demonstrated the NH tautomerism of NCPs by X-ray diffraction analyses of **I** and **II** (Figure 1).[6] Recently, "doubly *N*-confused porphyrins" and "doubly *N*-confused hexaphyrin"[7] have also been successfully synthesized.

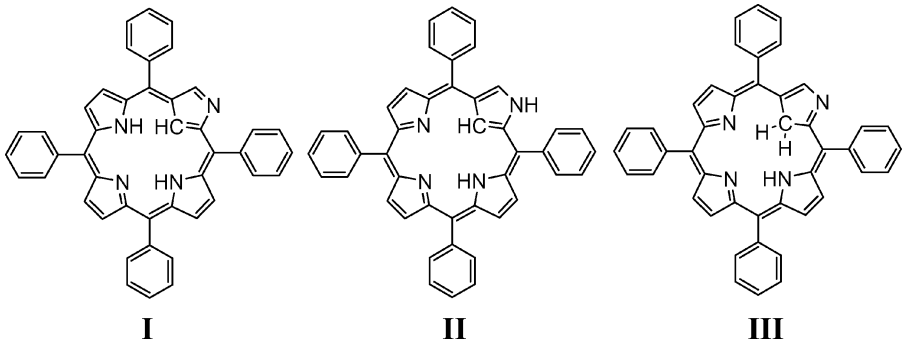

I **II** **III**

Figure 1. The tautomers (**I**, **II** and **III**) of *N*-confused porphyrin.

[a] Department of Chemistry and Center for Advanced Luminescence Materials, Hong Kong Baptist University, Kowloon Tong, Hong Kong, P. R. China
Fax: +852-3411-5862
E-mail: wkwong@hkbu.edu.hk

Due to its structural resemblance to normal porphyrins, NCP is expected to form complexes with a variety of metals. The unique coordination chemistry of NCP towards transition metals has been demonstrated progressively.[8] Important results include the non-traditional coordination modes of the NCP complexes,[8c,9] the stabilization of abnormal metal oxidation states,[10] the formation of metal–carbon bonds,[11] and the formation of dinuclear or polynuclear complexes through nitrogen coordination on an inverted pyrrole ring.[11e,12] However, related studies on lanthanide complexes of *N*-confused porphyrin have not yet been reported in detail due to their instability. We are interested in the chemistry and luminescent properties of lanthanide porphyrinate complexes. We[13] and others[14] have shown that the tripodal anion $(\eta^5\text{-}C_5H_5)Co[P(=O)(OMe)_2]_3^-$ (L^{OMe-}), is capable of stabilizing labile normal porphyrinate lanthanide(III) complexes by effectively encapsulating the lanthanide ion, thereby shielding it from interactions with the environment. We have extended our study to *N*-confused porphyrins and recently communicated the first lanthanide complexes of *N*-confused porphyrin with an η^2-agostic C–H interaction.[15] This further prompted us to explore the chemistry of lanthanide complexes of *N*-confused porphyrins in a systematic study, which could open a novel and interesting field, particularly for applications in catalysis. To this end, we have prepared a series of new lanthanide NCP complexes where both electron-donating and electron-withdrawing groups have been substituted at the *para*-position of the *meso* phenyl rings of *N*-confused porphyrin. We have also probed the effect of the substituent on the photophysical properties, such as absorption and visible and near-infrared fluorescence emissions, of the macrocycle.

Results and Discussion

Synthesis and Characterization of *N*-Confused Porphyrins

meso-Substituted *N*-confused porphyrin free-base (NCP) was synthesized by a Rothemund-type reaction,[16] which involves an acid-catalyzed pyrrole-aldehyde condensation and the concurrent formation of the normal porphyrin. Although the isolated yield reported in 1994 was low [*N*-confused tetraphenylporphyrin (H_2NCTPP, **1**): 5–7%[1] and *N*-confused tetratolylporphyrin (H_2NCTTP, **3**): 4%[2]], Lindsey et al. have improved the reaction yield to 39%.[5,17,18] We have synthesized a series of *meso*-substituted *N*-confused porphyrins, namely H_2NCTPP (**1**), H_2NCTTP (**2**), H_2NCTFPP (**3**), H_2NCTCPP (**4**), and H_2NCTTMSEPP (**5**), using an improved procedure, with yields of over 45% (Scheme 1).[19] All of these *N*-confused porphyrins were characterized by ^{1}H NMR spectroscopy and mass spectrometry. Compounds **1**–**5** exhibit the respective $[M + 1]^+$ peak in their FAB (positive mode) mass spectra, and a broad peak and a singlet at about δ = –2.50 and –5.10 ppm for the two NH protons and the inner CH proton, respectively, in their ^{1}H NMR spectra. They all exhibit two obvious tautomers, with a dramatic color change in the NCP solution.[6,9a] The photophysical properties of various substituted *N*-confused porphyrin free-bases have been fully studied by other groups.[19]

Synthesis and Characterization of Lanthanide Complexes of *N*-Confused Porphyrins

We have previously reported the synthesis of the cationic monoporphyrinate lanthanide complexes $[Ln(Por)(H_2O)_3]Cl$ by the reaction of $Ln[N(SiMe_3)_2]_3 \cdot x[LiCl(THF)_3]$ with porphyrin free-base in bis(methoxyethyl) ether. X-ray diffraction studies showed that the lanthanide ions are seven-coordinate and are surrounded by four N atoms from the porphyrin ring and three O atoms of the aqua ligands. These compounds readily form adducts with anionic tripodal ligands such as L_{OMe-} and hydridotris(pyrazole-1-yl)borate by a displacement reaction under mild conditions.[13] The *N*-confused porphyrins can also act as four-coordinate dianionic ligands, thereby enforcing coordination of the pyrrolic carbon to transition metal ions (e.g. Ni^{2+}).[11a] Upon complexation with lanthanide ions such as Yb^{3+} and Er^{3+}, X-ray diffraction studies revealed an η^2-agostic interaction between the Yb^{3+} ion and the inner C–H bond of the $NCTPP^{2-}$ ligand.[15] Similar to the normal porphyrins, the interaction of NCP free-bases with $Ln[N(SiMe_3)_2]_3 \cdot x[LiCl(THF)_3]$ (Ln = Yb^{3+} and Er^{3+}) gave the cationic NCP complexes $[(NCP)Ln(H_2O)_3]Cl$, which are unstable in air and could only be observed spectroscopically (by UV/Vis spectroscopy and mass spectrometry). However, when encapsulated with the tripodal anion L_{OMe-}, lanthanide *N*-

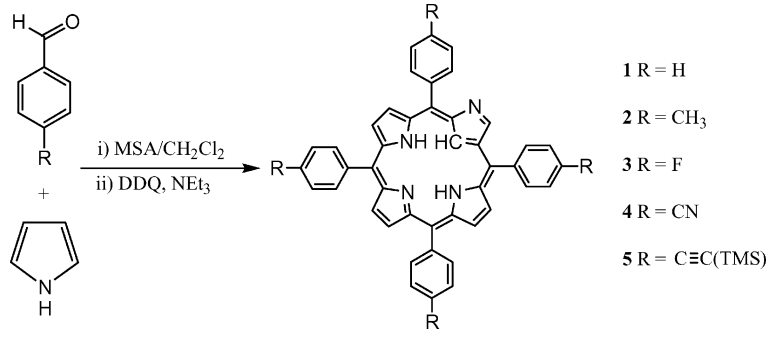

Scheme 1. Synthesis of *meso*-substituted *N*-confused porphyrins.

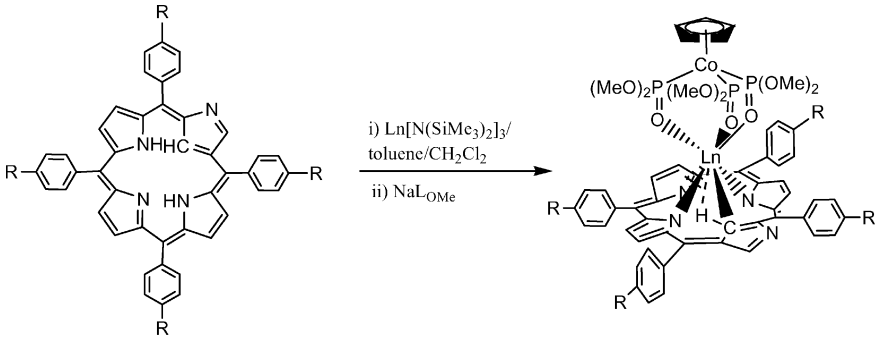

		Ln = Yb	Ln = Er
R = H	**1**	**6**	**11**
R = CH_3	**2**	**7**	**12**
R = F	**3**	**8**	**13**
R = CN	**4**	**9**	**14**
R = C≡CTMS	**5**	**10**	**15**

Scheme 2. Preparation of Ln^{III} complexes of *meso*-substituted *N*-confused porphyrins.

confused porphyrinate complexes of the general formula [(NCP)Ln(L_{OMe})] (**6**–**15**) could be obtained in 50–70% yields (Scheme 2). In a polar solvent, the lanthanide complexes of NCP with an electron-withdrawing group (**8**–**10**) are more stable than those with an electron-donating group (**6** and **7**).

The *N*-confused porphyrins and their lanthanide complexes were characterized by optical spectroscopy, mass spectrometry, elemental analysis, and IR and ^{1}H NMR spectroscopy, including 2D homo- and heteronuclear correlation techniques. All of the NCP complexes (**6**–**15**) gave satisfactory elemental analyses corresponding to the general formula [(NCP)Ln(L_{OMe})] and exhibited the $[M + 1]^+$ peak in their mass spectra. For instance, the electrospray ionization high resolution mass spectra (ESI-HRMS) of **8** and **9** exhibit the $[M + 1]^+$ peaks at *m*/*z* 1310.1306 and 1338.1558, respectively, which deviate less than 5 ppm from the theoretical values of 1310.1301 and 1338.1488, respectively; their isotopic distribution patterns match the theoretical distribution. The binding of a ligand to a paramagnetic Ln^{III} ion generally results in large NMR frequency shifts at the ligand nuclei, with magnitudes and signs depending critically on both the nature of the lanthanide ion and the location of the nucleus relative to the metal center.[20] For reasons of solubility and the strong paramagnetic effect of lanthanide ions on the NMR study, we selected only complexes **6**, **8**, and **9** for ^{1}H NMR characterization. The ^{1}H NMR spectrum of **6** consists of six distinct pairwise spin–spin-coupled broad signals at δ = –6.20, –5.48, –2.45, –1.58, 29.64, and 30.30 ppm corresponding to the β-H protons in different magnetic environments of the pyrroles, and a singlet at δ = 8.10 ppm for the unique α-H proton of the inverted pyrrole (Figures 2 and 3). In general, for a Ln complex with effective axial magnetic symmetry, the geometric factor (*G*) of the nucleus that contains the structural information about the complex inherent in the dipolar shift is given by $G = (3\cos^2\theta - 1)/r^3$, where *r* is the Ln–nucleus distance and θ is the angle between the Ln–nucleus vector and the main axis of symmetry of the magnetic susceptibility tensor of the complex.[21] Assuming that the structure in solution is the same as that determined in the solid state by X-ray crystallography, and based on the 2-D COSY ^{1}H NMR spectroscopic data, the resonance at δ = 37.99 ppm, which is substantially downfield shifted, was unambiguously assigned to the inner C–H proton of the NCTPP ligand. A large downfield shift of the inner C–H proton also indicates a strong interaction between the Yb^{3+} ion and this proton, which was also shown by the X-ray analysis to be an agostic interaction (see below and ref.[14]). Complexes **8** and **9** display a similar ^{1}H NMR pattern. For complex **8** (**9**), the six β-H protons appear at δ = –6.21, –5.47, –2.10, –1.49, 29.67 and 30.16 ppm (δ = –6.08, –5.31, –2.05, –1.23, 29.64 and 29.98 ppm), the unique α-H proton at δ = 8.19 ppm (δ = 8.30 ppm), and the inner C–H proton of NCP at δ = 37.74 ppm (δ = 37.41 ppm). The ^{31}P{^{1}H} NMR spectra of the lanthanide(III) NCP complexes show a single peak at around δ = 78.0–82.8 ppm for the Yb^{III} complexes (**6**–**10**) and δ = –123.2 to –128.8 ppm for the Er^{III} complexes (**11**–**15**) for the phosphito groups of the anionic L_{OMe^-} ligand. The IR spectra of NCTCPP (**9** and **14**) and NCTTMSEPP (**10** and **15**) complexes exhibit the $\nu_{C\equiv N}$ and $\nu_{C\equiv C}$ bands at around 2225 and 2156 cm^{-1}, respectively.

When the [(NCP)Ln(L_{OMe})] complexes were treated with an excess amount of methyl iodide in the presence of Cs_2CO_3, the *N*-methylated complexes [(*N*-Me-NCP)-Ln(L_{OMe})]$^+I^-$, in which the unique peripheral nitrogen of the NCP is methylated, were obtained in almost quantitative yields (Scheme 3). For instance, when complex **9** was treated with an excess amount of methyl iodide in the presence of Cs_2CO_3, the *N*-methylated complex [(*N*-Me-NCTCPP)Ln(L_{OMe})]$^+I^-$ (**16**) was isolated. Complex **16** was characterized by elemental analyses and spectroscopic techniques. It exhibits the $[M - I]^+$ peak at *m*/*z* 1352.1680 (vs. the theoretical value of 1352.1639 amu) in the ESI-HRMS, a single peak at δ = 83.2 ppm in the ^{31}P NMR spectrum, and the $\nu_{C\equiv N}$ signal at $\tilde{\nu}$ = 2227 cm^{-1} in the IR spectrum. Based on the 2-D COSY ^{1}H NMR spectroscopic data, the resonance at δ = 41.64 ppm was assigned to the inner C–H

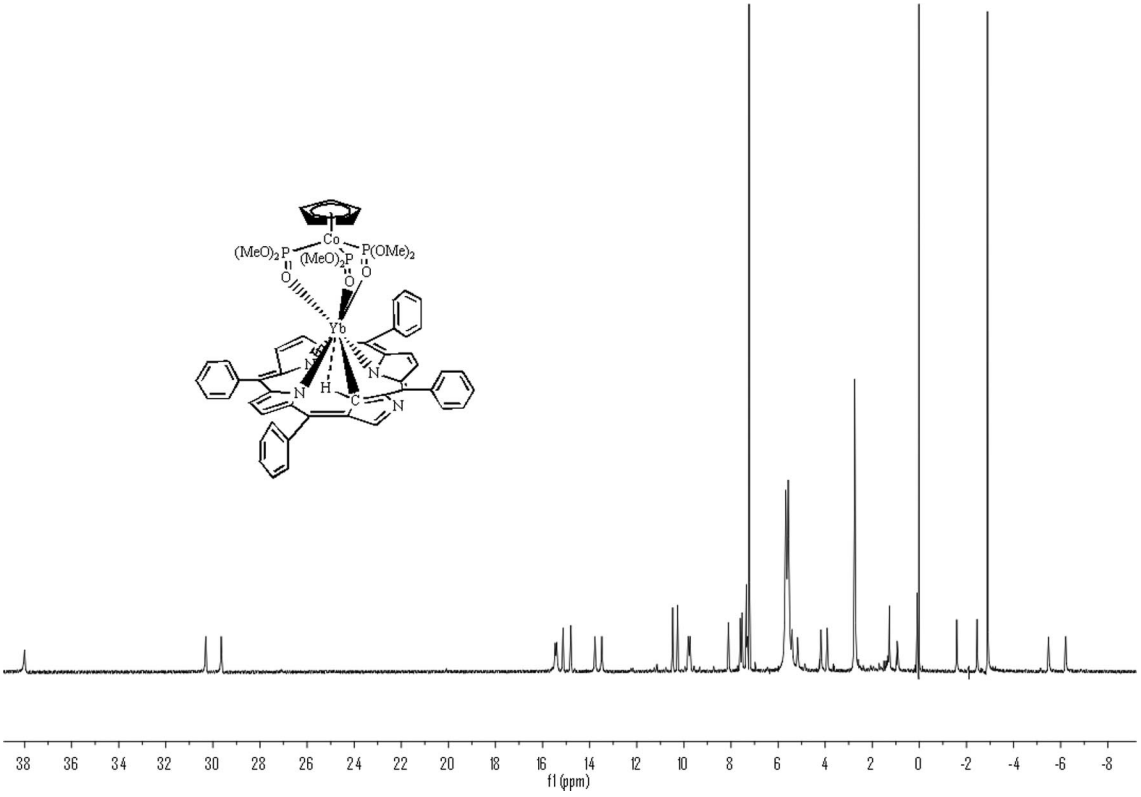

Figure 2. ^{1}H NMR spectrum of complex **6** in $CDCl_3$.

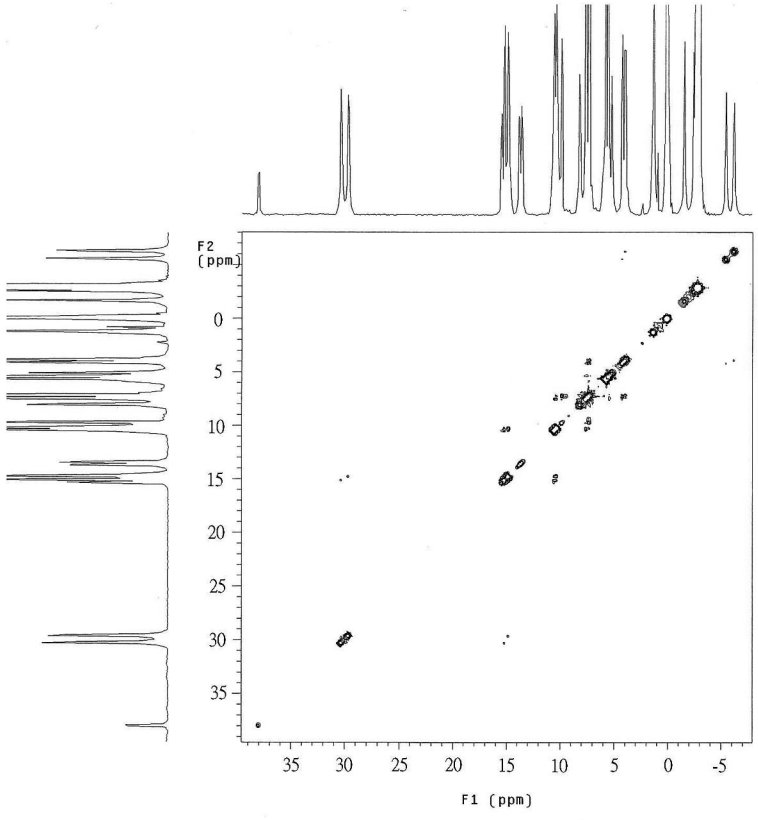

Figure 3. 2D COSY ^{1}H NMR spectrum of complex **6** in $CDCl_3$.

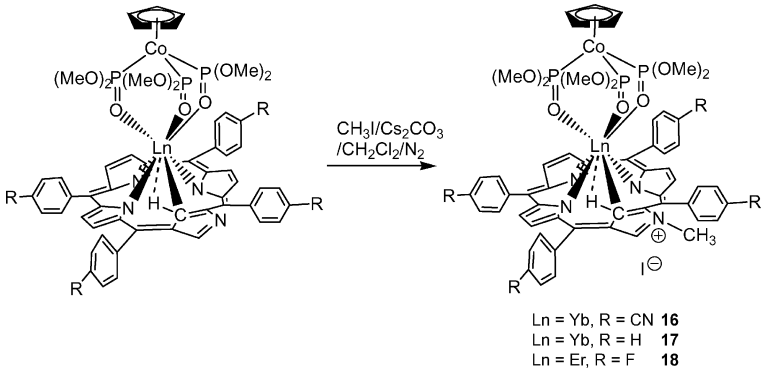

Scheme 3. Preparation of $[(N\text{-Me-NCP})Ln(L_{OMe})]^{+}I^{-}$.

proton of the NCP ligand. The substantially downfield shifted resonance of the inner C–H proton indicates that the NCP complex still retains the agostic interaction between the Yb^{3+} ion and the inner C–H bond upon methylation at the peripheral nitrogen, as subsequently indicated by X-ray crystallography (see below).

X-ray Crystal Structures of Lanthanide Complexes of *N*-Confused Porphyrins

The solid-state structures of **8** (Figure 4), **9** (Figure 5), and **13** (Figure 6) were ascertained by X-ray crystallography. These complexes are structurally quite similar around the metal core. Selected bond lengths and angles are given in Table 1. We were able to locate the hydrogen atom in the inner core C–H group on C(2) for **8** and C(5) for both **9** and **13** from the Fourier difference maps. In each case, the overall structure of the NCP dianion adopts a nonplanar geometry with an inverted pyrrole ring tilted away from the metal and the porphyrin plane defined by the three inner pyrrolic N atoms. The three regular pyrroles are slightly distorted, with mean deviations of 0.2207, 0.1991, and 0.2176 Å from the plane defined by 19 atoms on the pyrrole rings and methine carbons for **8**, **9**, and **13**, respectively. The Yb^{3+} ion is eight-coordinate and is bonded to the NCP^{2-} and L_{OMe^-} ligands. Other than coordinating to the three O atoms of the L_{OMe^-} ligand, the Yb^{3+} ion is also bound to the three inner N atoms and forms an η^2-agostic bond with the inner C–H edge of the NCP ligand. The Yb center sits 1.2881 and 1.2572 Å above the mean plane of the macrocycle in **8** and **9**, respectively. The Yb–N and Yb–O distances for **8** (**9**) are in the range 2.300(6)–2.419(7) Å

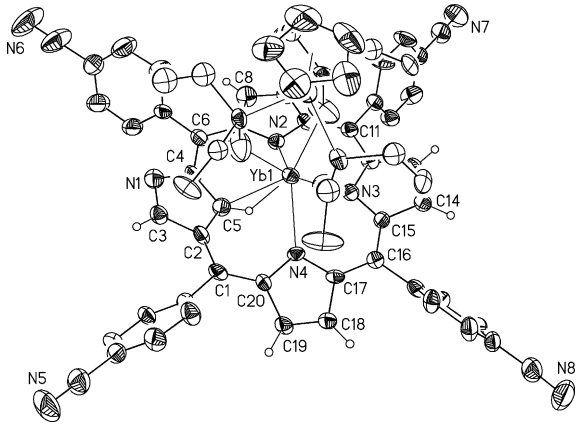

Figure 5. A perspective view of complex **9**. Only hydrogen atoms on the pyrrole ring are shown for clarity.

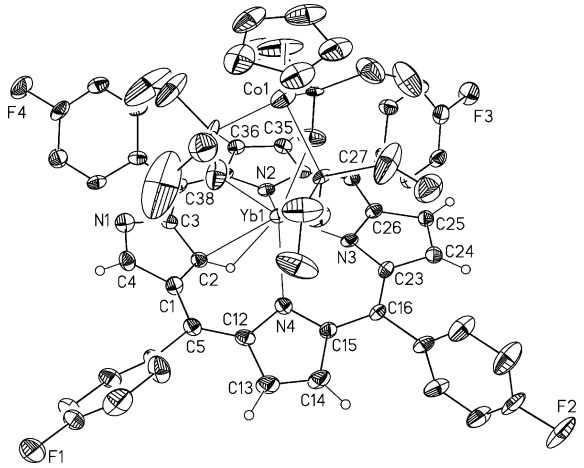

Figure 4. A perspective view of complex **8**. Only hydrogen atoms on the pyrrole ring are shown for clarity.

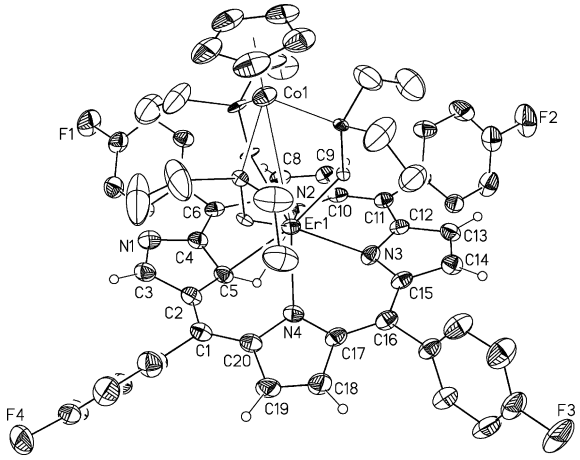

Figure 6. A perspective view of complex **13**. Only hydrogen atoms on the pyrrole ring are shown for clarity.

[2.341(5)–2.415(6) Å] and 2.186(5)–2.240(4) Å [2.220(8)–2.236(7) Å], respectively, and are comparable to those reported for normal lanthanide monoporphyrinate complexes.[13] The Er–N and Er–O bond lengths in **13** are within the range 2.343(5)–2.421(5) and 2.230(6)–2.272(6) Å, respectively. The Yb(1)–C distance of 2.643(8) Å for **8**, 2.553(7) Å for **9**, and 2.581(6) Å for **13** is much longer than the Yb–C bond length [2.388(4) Å] reported in the literature.[22] For **8**, in addition to the relatively short C(2)–C(3) and C(4)–N(1) bond lengths of 1.38(1) and 1.34(1) Å, respectively, the bond angles of 107.7(7)° for N(1)–C(3)–C(2) and 108.1(7)° for C(3)–N(1)–C(4) are consistent with the tautomer form **I**.[6] A similar observation was also noted for **9** and **13** (see Table 1). The distance from Ln^{3+} to the inner core hydrogen is only 2.643, 2.577, and 2.497 Å for **8**, **9**, and **13**, respectively, with the inner C–H distance being 0.957–0.982 Å. These values are consistent with the bond length of an agostic interaction. This seems to be in line with the effect due to the coordinatively unsaturated and electron-deficient Ln center, which results in a stronger three-center two-electron C–H···Ln contact. A solid-state packing effect could also lead to such an interaction. The much shorter Ln(1)–N(3) distance [2.300(6), 2.341(5), and 2.343(5) Å for **8**, **9**, and **13**, respectively] *trans* to the inverted pyrrole ring suggests a stronger electron-donating ability of this pyrrolic N atom to the relatively electron-deficient lanthanide ion center and further supports an agostic interaction between the metal and inner core C–H bond.[15] A similar agostic interaction between a transition metal ion and an inner C–H bond of NCP has been observed in other systems.[9] The agostic interaction between the C–H bond and the Ln^{3+} ion may contribute to the stabilization of these lanthanide NCTPP complexes to some extent.

The solid-state structure of **16** was also determined by X-ray crystallography; a perspective view is depicted in Figure 7. Selected bond lengths and angles are given in Table 1. The structural analysis of **16** revealed that other than having a methyl group attached to the peripheral nitrogen N(1), its core structure is very similar to that of the precursor complex **9**. The *N*-Me-NCTCPP dianion adopts a nonplanar geometry (with a mean deviation of 0.1223 Å from

Table 1. Selected bond lengths [Å] and angles [°] for compounds **8**, **9**, **13**, and **16**.

	8		
Yb(1)–N(2)	2.406(6)	Yb(1)–N(3)	2.300(6)
Yb(1)–N(4)	2.419(7)	Yb(1)–O(1)	2.246(7)
Yb(1)–O(2)	2.206(7)	Yb(1)–O(3)	2.183(7)
Yb(1)–C(2)	2.643(8)	C(2)–C(3)	1.38(1)
C(1)–C(2)	1.42(1)	C(3)–N(1)	1.41(1)
C(4)–N(1)	1.34(1)	C(1)–C(4)	1.41(1)
C(1)–C(5)	1.43(1)	C(2)–H(2)	0.963
Yb(1)···H(2)	2.643		
N(2)–Yb(1)–N(3)	76.8(2)	N(3)–Yb(1)–N(4)	76.5(2)
N(4)–Yb(1)–N(2)	120.3(2)	O(1)–Yb(1)–N(4)	150.2(3)
O(1)–Yb(1)–N(3)	86.9(2)	O(2)–Yb(1)–N(3)	167.1(3)
O(1)–Yb(1)–N(2)	78.4(2)	O(2)–Yb(1)–N(2)	103.0(3)
O(3)–Yb(1)–N(4)	77.5(3)	O(3)–Yb(1)–N(3)	91.8(2)
O(3)–Yb(1)–N(2)	154.7(3)	C(3)–C(2)–Yb(1)	104.9(5)
C(1)–C(2)–Yb(1)	104.8(5)	C(1)–C(4)–N(1)	110.7(7)
C(3)–C(2)–C(1)	108.3(7)	C(4)–N(1)–C(3)	108.1(7)
	9		
Yb(1)–N(2)	2.415(6)	Yb(1)–N(3)	2.341(5)
Yb(1)–N(4)	2.387(5)	Yb(1)–O(1)	2.231(7)
Yb(1)–O(2)	2.236(7)	Yb(1)–O(3)	2.220(8)
Yb(1)–C(5)	2.553(7)	C(2)–C(5)	1.430(11)
C(2)–C(3)	1.450(10)	C(4)–C(5)	1.385(10)
C(3)–N(1)	1.329(11)	C(4)–N(1)	1.428(10)
C(5)–H(1)	0.957	Yb(1)···H(1)	2.577
N(2)–Yb(1)–N(3)	76.8(2)	N(3)–Yb(1)–N(4)	76.16(19)
N(4)–Yb(1)–N(2)	121.5(2)	O(1)–Yb(1)–N(4)	113.1(3)
O(1)–Yb(1)–N(3)	167.0(2)	O(2)–Yb(1)–N(3)	85.4(2)
O(1)–Yb(1)–N(2)	104.1(3)	O(2)–Yb(1)–N(2)	79.2(3)
O(3)–Yb(1)–N(4)	76.0(2)	O(3)–Yb(1)–N(3)	93.6(3)
O(3)–Yb(1)–N(2)	156.0(2)	C(4)–C(5)–Yb(1)	109.1(5)
C(2)–C(5)–Yb(1)	106.7(5)	C(4)–N(1)–C(3)	106.0(6)
C(4)–C(5)–C(2)	106.8(6)	N(1)–C(3)–C(2)	111.8(7)
	13		
Er(1)–N(2)	2.401(4)	Er(1)–N(3)	2.343(5)
Er(1)–N(4)	2.421(5)	Er(1)–C(5)	2.581(6)
Er(1)–O(1)	2.272(6)	Er(1)–O(2)	2.230(6)
Er(1)–O(3)	2.265(6)	C(2)–C(5)	1.415(9)
C(4)–C(5)	1.389(9)	C(3)–N(1)	1.311(8)
C(4)–N(1)	1.416(9)	C(5)–H(5)	0.982
Er(1)···H(5)	2.497		
N(2)–Er(1)–N(3)	76.55(17)	N(3)–Er(1)–N(4)	75.21(18)
N(4)–Er(1)–N(2)	120.32(16)	C(4)–C(5)–Er(1)	106.4(4)
C(4)–C(5)–C(2)	107.5(6)	N(1)–C(3)–C(2)	111.5(6)
C(3)–N(1)–C(4)	107.6(6)		
	16		
Yb(1)–N(2)	2.460(6)	Yb(1)–N(3)	2.344(4)
Yb(1)–N(4)	2.390(5)	Yb(1)–O(1)	2.155(8)
Yb(1)–O(2)	2.184(6)	Yb(1)–O(3)	2.188(7)
Yb(1)–C(48)	2.601(7)	C(2)–C(48)	1.398(9)
C(47)–C(48)	1.387(9)	C(47)–C(49)	1.362(8)
C(1)–N(1)	1.433(12)	C(2)–N(1)	1.368(8)
C(49)–N(1)	1.371(10)	C(48)–H(48)	0.974
Yb(1)···H(48)	2.679		
N(2)–Yb(1)–N(3)	75.08(17)	N(3)–Yb(1)–N(4)	75.25(16)
N(4)–Yb(1)–N(2)	116.27(19)	C(47)–C(48)–Yb(1)	108.7(5)
C(2)–C(48)–Yb(1)	110.7(4)	C(49)–N(1)–C(2)	109.9(6)
C(47)–C(48)–C(2)	108.5(5)	N(1)–C(2)–C(48)	105.9(6)

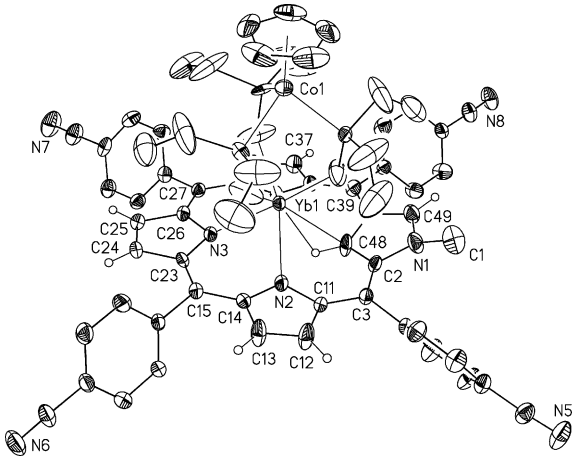

Figure 7. A perspective view of complex **16**. Only hydrogen atoms on the pyrrole ring are shown for clarity.

the plane) with an inverted pyrrole ring tilted away from the metal and the porphyrin plane defined by N(2), N(3), and N(4). The Yb center sits 1.3478 Å above the mean plane of the NCP ring. The Yb^{3+} ion is eight-coordinate and is bonded to the *N*-Me-NCTCPP^{2-} and L_{OMe^-} ligands. Other than coordinating to the three O atoms of the L_{OMe^-} ligand, the Yb^{3+} ion is also bound to the three inner N atoms and forms an η^2-agostic bond with the inner C–H edge of the NCTCPP ligand. The Yb–N and Yb–O distances are in the ranges 2.344(4)–2.460(6) and 2.155(8)–2.188(7) Å, respectively, and are comparable to those in **9**. The Yb(1)–C(48) distance of 2.601(7) Å compares well with the Yb–C bond length in **9** and that in a similar lanthanide complex [(NCTPP)Ln(L_{OMe})] [2.601(4) Å] reported previously.[15] In addition to the relatively short C(2)–C(48) and C(49)–N(1) bond lengths [1.398(9) and 1.37(1) Å, respectively], the bond angles of 105.9(6)° for N(1)–C(2)–C(48) and 109.9(6)° for C(2)–N(1)–C(49) are consistent with the most stable tautomeric form (**I**) of NCP.[6] The Yb(1)···H distance is 2.679 Å, thus confirming the retention of an agostic interaction even after methylation.

Photophysical Properties of Lanthanide *N*-Confused Porphyrinate Complexes

The ability of Yb^{3+} and Er^{3+} ions to emit in the near-infrared (NIR) region renders them interesting for diagnostic or tagging applications.[23–25] As the direct excitation of lanthanide ions is more demanding due to the forbidden optical transitions within 4f subshells, much effort has been devoted to the synthesis of complexes possessing the appropriate antenna.[25] We have reported previously on the photoluminescent properties of Yb^{III} and Er^{III} monoporphyrinate complexes.[13d,26,27] The results reveal that the porphyrin ring, as an antenna, can absorb and transfer energy to the lanthanide ions when irradiated by visible light and lead to the emission of lanthanide ions in the NIR region. We therefore investigated the luminescent properties of the newly synthesized lanthanide *N*-confused porphyrinate complexes, paying particular attention to their NIR emission properties in toluene. The photophysical properties of the lanthanide *N*-confused porphyrinate complexes **6**–**15** are summarized in Table 2. At room temperature, the solution electronic absorption and emission spectra of these lanthanide complexes in the UV/Vis region are red-shifted relative to those of the lanthanide normal porphyrinate complexes and are characteristic of intra-ligand transitions.[28a] The absorption bands of **6**, **7**, **11**, and **12** are characterized by significantly red-shifted Soret band and Q-band absorptions at around 459, 670, and 722 nm. Complexes **8** and **13**, which contain a *para*-fluorophenyl *meso*-substituted NCP, exhibit almost the same red-shifted Soret band at 459 nm but only one broad Q-band at 670 nm. The presence of a cyano or alkynyl group results in a more intense red-shifted Soret band and broad Q-band absorptions at about 469 and 677 nm for **9**, **10**, **14**, and **15**.

Figure 8 shows the absorption spectra of **6** and **9**. The fluorescence spectra of lanthanide complexes of NCP are characterized by emission bands that are red-shifted relative to those of the lanthanide complexes of normal porphyrins.[26,27] The emission peaks at about 690 and 760 nm can be assigned to the intra-ligand $\pi \rightarrow \pi^*$ transitions of the NCP ligand (Figures 9 and 10). The quantum efficiencies and fluorescence lifetimes of Yb^{3+} and Er^{3+} complexes of NCP are also different from each other and from those of

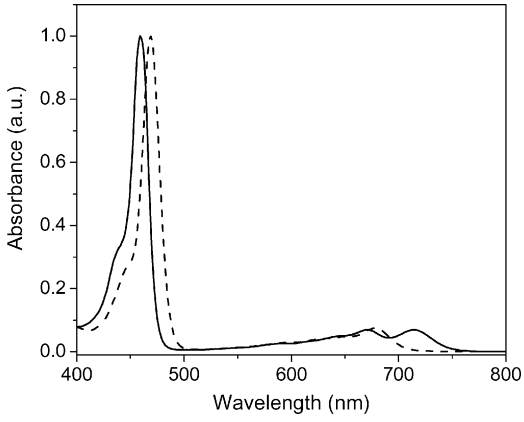

Figure 8. Normalized absorption spectra of Yb^{3+} complexes **6** (solid line) and **9** (dashed line) in toluene at room temperature.

Table 2. Summary of absorption and fluorescence data for complexes **6**–**16**.

Compound	Absorption λ_{max} [nm] ($\log \varepsilon$ [$M^{-1}\,cm^{-1}$])[a]	Excitation λ_{exc} [nm]	Emission λ_{em} [nm] (τ, $\Phi_{em} \times 10^3$)[b,c]
6	459 (5.68), 670 (4.53), 714 (4.53)	462	689 (0.96 ns, 0.17), 730, 980 (0.26 μs)
7	460 (5.44), 673 (4.30), 722 (4.30)	465	692 (1.0 ns, 0.25), 743, 980 (0.19 μs)
8	459 (5.53), 670 (4.31)	460	687 (0.98 ns, 0.18), 980 (0.28 μs)
9	469 (5.46), 679 (4.33)	468	689 (1.0 ns, 1.17), 978 (0.35 μs)
10	469 (5.56), 681 (4.53)	447	703 (4.71 ns, 0.5), 760, 980 (0.38 μs)
11	459 (5.46), 670 (4.28), 714 (4.28)	440	687 (1.01 ns, 0.49), 748, 1581
12	460 (5.44), 672 (4.30), 721 (4.30)	462	690 (1.01, 0.52), 747, 1572
13	458 (5.53), 670 (4.31)	461	687 (1.02 ns, 0.44), 1566
14	469 (5.42), 678 (4.31)	469	697 (1.01 ns, 0.82), 1577
15	469 (5.58), 680 (4.54)	448	702 (6.18 ns, 0.63), 760, 1577
16	468 (5.46), 748 (4.86)	450	738 (4.11 ns, 0.81), 980 (0.32 μs)

[a] Photophysical measurements were made in toluene solution at room temperature. [b] The quantum yield standard used in this study was H_2TPP in outgassed anhydrous benzene (Φ_F = 0.11 at 298 K).[29b] [c] Due to the limitations of the instrument, we were unable to determine the quantum yields of the NIR luminescence of these compounds.

the free NCP, with the quantum yield for **9** (Φ_{F1} = 0.00117) being greater than that for **6** (Φ_{F1} = 0.00017) by a factor of 10. These values are much lower than that for the corresponding NCP free-base (Φ_{F1} = 0.023 for H_2NCTPP **1**)[20] or the normal porphyrin free-base (Φ_{F1} = 0.11 for tetraphenylporphyrin, H_2TPP).[28b] These lanthanide NCP complexes also exhibit an emission band corresponding to the Ln^{3+} ion emission in the NIR region (Figure 11). For the Yb^{3+} NCP complexes, the emission peaks centered at around 980 nm can be assigned to the $^2F_{5/2} \rightarrow {}^2F_{7/2}$ transition of the Yb^{3+} ion and show a lifetime ranging from 0.19 to 0.38 μs, which is much longer than the porphyrinate singlet exited state fluorescence decay.

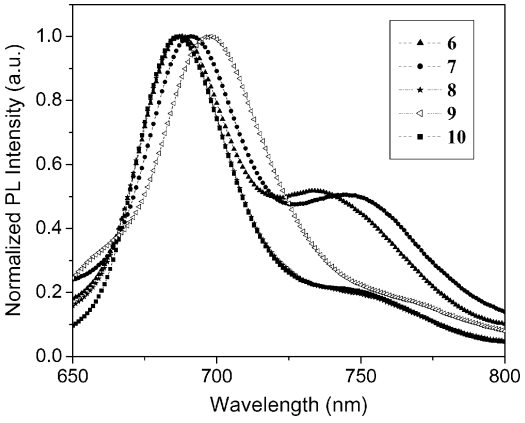

Figure 9. Normalized emission spectra of Yb^{3+} complexes **6**–**10** upon excitation at 460 nm at a concentration of about 1×10^{-6} M in toluene.

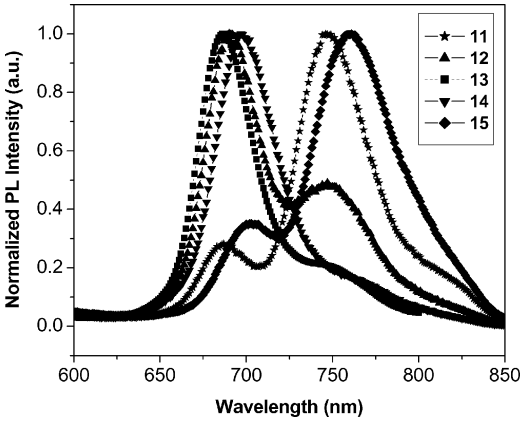

Figure 10. Normalized emission spectra of Er^{3+} complexes **11**–**15** upon excitation at 460 nm at a concentration of about 1×10^{-6} M in toluene.

It has been shown that the C–H vibration may quench the NIR emission of Ln^{3+} ions.[29] Indeed, the intensity of the NIR emission of [Yb(NCTPP)(L_{OMe})] is at least an order of magnitude weaker than the corresponding normal porphyrinate complex [Yb(TPP)(L_{OMe})] (TPP^{2-} = 5,10,15,20-tetraphenylporphyrinate dianion).[13] This provides further evidence for the presence of an η^2-agostic interaction between the Yb^{3+} ion and the inner C–H bond of the $NCTPP^{2-}$ ligand. For the Er^{3+} NCP complexes, weak

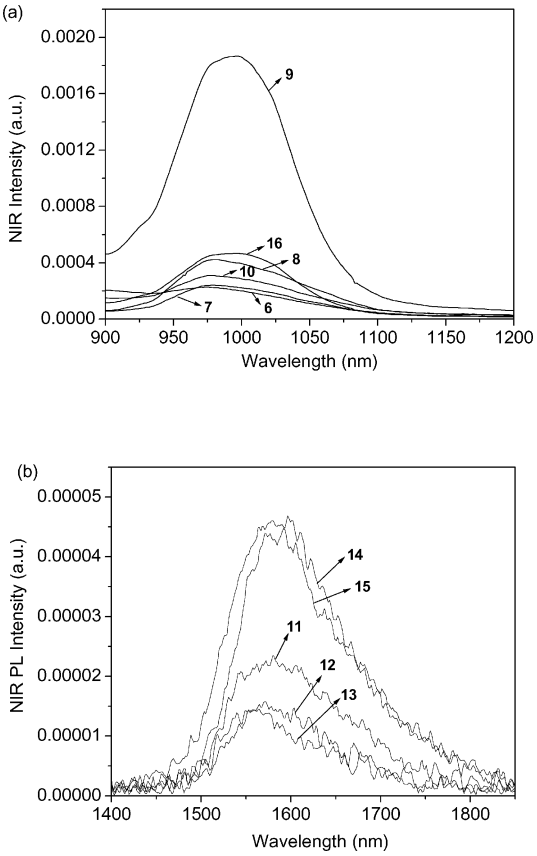

Figure 11. Emission spectra of (a) Yb^{3+} and (b) Er^{3+} complexes upon excitation at 514 nm at a concentration of about 1×10^{-6} in toluene at room temperature (note that the transitions are $^2F_{5/2} \rightarrow {}^2F_{7/2}$ for Yb^{3+} and $^4I_{13/2} \rightarrow {}^4I_{15/2}$ for Er^{3+}).

emission peaks centered at about 1570 nm are observed. These can be attributed to the $^4I_{13/2} \rightarrow {}^4I_{15/2}$ transition of Er^{3+} ion.

The absorption spectrum of complex **16** in toluene displays a Soret band and a Q-band at 468 and 748 nm, respectively. The Q-band is substantially red-shifted relative to that of the non-methylated complex **9**, for which it is located at 678 nm (Figure 12). These spectral features resemble those observed for a related methylated nickel(II)

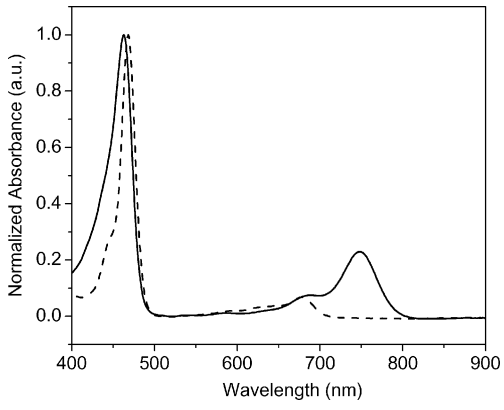

Figure 12. Normalized UV/Vis spectra of **9** (dashed line) and **16** (solid line) in toluene.

complex.[11a] Other than the intra-ligand visible emission, complex **16** also exhibits an NIR emission of the Yb^{3+} ion at about 980 nm, whose intensity is much weaker than that of **9** (Figure 9, a).

Conclusions

Lanthanide(III) complexes of *N*-confused porphyrins containing various rare earth metals and phenyl ring substituents, in which the tripodal cobaltate anion acts as an effective encapsulating agent for Ln^{3+} and an η^2-agostic interaction exists between the metal center and the inner C–H bond of the porphyrinate ligand, have been synthesized. The crystal structures and photophysics of these new complexes and their methylated congeners have been examined.

Experimental Section

General: All reagents and solvents were of the commercial reagent grade and were used without further purification except where noted. Dichloromethane was distilled from calcium hydride. Toluene and THF were distilled under nitrogen in the presence of sodium chips using benzophenone ketyl as an indicator. The freshly distilled solvents were bubbled with nitrogen for at least 10 min to remove the residual oxygen. Pyrrole was freshly distilled from calcium hydride before use. Elemental analyses (C, H, N) were performed by the Shanxi University, P.R. China. NMR spectra were recorded with a JEOL EX270 spectrometer. Chemical shifts of the ^1H NMR spectra were referenced to internal deuterated solvents and then recalculated to $SiMe_4$ (δ = 0.00 ppm) and $^{31}P\{^1H\}$ NMR spectra to external 85% H_3PO_4. Electrospray ionization high-resolution mass spectra (ESI-HRMS) were recorded with a QSTAR mass spectrometer, the UV/Vis absorption spectra with a Hewlett–Packard 8453 UV/Vis spectrophotometer, the steady-state visible fluorescence and PL excitation spectra with a Photon Technology International (PTI) Alphascan spectrofluorimeter and visible decay spectra with a pico-N_2 laser system (PTI Time Master) at an excitation wavelength of 337 nm. Quantum yields of visible emissions were computed according to the literature method[30] using H_2TPP in outgassed anhydrous benzene as the reference standard (Φ_F = 0.11 at 298 K).[28b] The NIR emission was detected by a liquid-nitrogen-cooled InSb IR detector (EG & G) with a preamplifier and recorded by a lock-in amplifier system. The third harmonics, 355-nm line of a Nd:YAG laser (Quantel Brilliant B), was used as the excitation light source.

General Procedure for the Preparation of *meso*-Substituted *N*-Confused Porphyrins: Methanesulfonic acid (MSA) (0.34 mL, 5.2 mmol) was added to a solution of pyrrole (0.52 mL, 7.5 mmol) and aryl aldehyde (7.5 mmol) in CH_2Cl_2 (750 mL). The mixture was stirred for 30 min, then 2,3-dichloro-5,6-dicyano-1,4-benzoquinone (DDQ; 1.5 g, 6.6 mmol) was added, followed, after 1 min, by triethylamine (1.5 mL). The crude mixture was chromatographed with a silica gel column eluting with CH_2Cl_2/methanol (100/1, v/v) after filtration of the crude reaction mixture through a pad of basic alumina. A pure sample of each NCP for the ^1H NMR analysis was obtained by recrystallization from a CH_2Cl_2/methanol mixture.

H_2NCTPP (1): Yield 379 mg (33%); m.p. > 300 °C (dec.). ^1H NMR ($CDCl_3$): δ = 8.98 (d, *J* = 4.8 Hz, 1 H), 8.91 (d, *J* = 4.8 Hz, 1 H), 8.76 (s, 1 H), 8.62–8.55 (m, 4 H, β-H), 8.38–8.31 (m, 4 H, Ar-H), 8.16–8.15 (m, 4 H, Ar-H), 7.83–7.75 (m, 12 H, Ar-H), –2.50 (br., 2 H, NH), –5.00 (s, 1 H, CH) ppm. FAB-MS: *m*/*z* 615.5 [M + 1]$^+$; $C_{44}H_{31}N_4$ requires 615.2. UV/Vis (toluene, 20 °C): λ_{max} (log ε) = 438 nm (5.20 $M^{-1}cm^{-1}$), 539 (3.89), 580 (4.03), 724 (4.01).

H_2NCTTP (2): Yield 390 mg (31%); m.p. > 300 °C (dec.). ^1H NMR ($CDCl_3$): δ = 8.93 (d, *J* = 4.8 Hz, 1 H), 8.87 (d, *J* = 4.8 Hz, 1 H), 8.71 (s, 1 H), 8.56–8.54 (m, 4 H, β-H), 8.25 (d, *J* = 8.0 Hz, 2 H, Ar-H), 8.20 (d, *J* = 8.0 Hz, 2 H, Ar-H), 8.02 (t, *J* = 8.0 Hz, 4 H, Ar-H), 7.63 (d, *J* = 8.0 Hz, 4 H, Ar-H), 7.52 (dd, *J* = 2.0, *J* = 8.0 Hz, 4 H, Ar-H), 2.67 (t, *J* = 4.8 Hz, 12 H, CH_3), –2.5 (br., 2 H, NH), –5.01 (s, 1 H, CH) ppm. FAB-MS: *m*/*z* 671.9 [M + 1]$^+$; $C_{48}H_{39}N_4$ requires 671.8. UV/Vis (toluene, 20 °C): λ_{max} (log ε) = 442 (5.16), 544 (3.94), 587 (4.14), 731 (3.96).

H_2NCTFPP (3): Yield 450 mg (35%); m.p. > 300 °C (dec.). ^1H NMR ($CDCl_3$): δ = 8.93 (d, *J* = 4.8 Hz, 1 H), 8.87 (d, *J* = 4.8 Hz, 1 H), 8.71 (s, 1 H), 8.56–8.54 (m, 4 H, β-H), 8.25 (d, *J* = 8.0 Hz, 2 H, Ar-H), 8.20 (d, *J* = 8.0 Hz, 2 H, Ar-H), 8.02 (t, *J* = 8.0 Hz, 4 H, Ar-H), 7.63 (d, *J* = 8.0 Hz, 4 H, Ar-H), 7.52 (d, *J* = 8.0 Hz, 4 H, Ar-H), –2.50 (br., 2 H, NH), –5.01 (s, 1 H, CH) ppm. FAB-MS: *m*/*z* 687.5 [M + 1]$^+$; $C_{44}H_{27}F_4N_4$ requires 687.2. UV/Vis (toluene, 20 °C): λ_{max} (log ε) = 440 (4.97), 541 (3.80), 584 (3.92), 727 (3.72).

H_2NCTCPP (4): Yield 509 mg (38%); m.p. > 300 °C (dec.). ^1H NMR ($CDCl_3$): δ = 8.97 (d, *J* = 4.8 Hz, 1 H), 8.92 (d, *J* = 4.8 Hz, 1 H), 8.71 (s, 1 H), 8.62–8.42 (m, 8 H, β-H and Ar-H), 8.28 (m, 4 H, Ar-H), 8.20–8.08 (m, 8 H, Ar-H), –2.5 (br., 2 H, NH), –5.11 (s, 1 H, CH) ppm. ESI-HRMS (in methanol, positive mode): *m*/*z* 715.2405 [M + 1]$^+$; $C_{48}H_{27}N_8$ requires 715.2358 (deviation 6.57 ppm). UV/Vis (toluene, 20 °C): λ_{max} (log ε) = 444 (5.02), 543 (4.00), 587 (4.09), 726 (3.99). IR (KBr): $\nu_{C\equiv N}$ = 2225 cm^{-1}.

H_2NCTTMSEPP (5): Yield 655 mg (35%); m.p. > 300 °C (dec.). ^1H NMR ($CDCl_3$): δ = 8.87 (d, *J* = 4.8 Hz, 1 H), 8.65 (m, 2 H), 8.45 (d, *J* = 4.8 Hz, 1 H), 8.34 (m, 4 H), 8.18 (dd, *J* = 8.0, *J* = 11.2 Hz, 4 H), 7.98 (dd, *J* = 2.4, *J* = 8.0 Hz), 7.93 (dd, *J* = 8.0, *J* = 11.2 Hz), 7.84 (d, *J* = 8.0 Hz, 4 H), 0.35 (m, 36 H), –2.50 (br., 2 H), –5.33 (s, 1 H) ppm. FAB-MS: *m*/*z* 999.6 [M + 1]$^+$; $C_{64}H_{63}N_4Si_4$ requires 999.4. UV/Vis (toluene, 20 °C): λ_{max} (log ε) = 448 (5.28), 551 (3.81), 592 (4.19), 734 (3.93). IR ($\nu_{C\equiv C}$, in KBr): $\tilde{\nu}$ = 2156 cm^{-1}.

Preparations of [(NCP)Ln(L_{OMe})] (Ln = Yb and Er)

$Yb[N(SiMe_3)_2]_3{\cdot}[LiCl(THF)_3]_x$ (A): $HN(SiMe_3)_2$ (10.8 mL, 0.050 mol) was dissolved in 20 mL of THF in an ice bath. *n*BuLi (1.6 M in hexane; 31.0 mL, 0.050 mol) was then added slowly over a period of 30 min. The resulting solution was magnetically stirred for 12 h until a clear, pale-yellow solution was obtained. The solution was transferred slowly to a Schlenk flask containing $YbCl_3$ (4.74 g, 0.017 mol) suspended in 20 mL of THF. The resulting mixture was magnetically stirred for 24 h until all of the solid $YbCl_3$ had disappeared. The resulting solution **A** contains $Yb[N(SiMe_3)_2]_3{\cdot}[LiCl(THF)]_x$ (*x* = 3–5).

$Er[N(SiMe_3)_2]_3{\cdot}[Li(THF)Cl]_x$ (B): $Er[N(SiMe_3)_2]_3{\cdot}[LiCl(THF)]_x$ (*x* = 3–5) was prepared by the same method as solution **A** except that $HN(SiMe_3)_2$ (10.8 mL 0.050 mol), *n*BuLi (1.6 M in hexane; 31.0 mL, 0.050 mol) and $ErCl_3$ (4.65 g, 0.017 mol) in THF were used.

General Procedure for the Preparation of Lanthanide Complexes of *meso*-Substituted *N*-Confused Porphyrin. Synthesis of [(NCP)Yb(L_{OMe})]: Solution **A** (2.5 mL, 0.52 mmol Yb), prepared as above, was transferred into a Schlenk flask and the solvent removed under vacuum. Dichloromethane (10 mL) was then added to precipitate LiCl. The mixture was centrifuged and the clear layer transferred to another Schlenk flask containing dry NCP (0.16 mmol) dissolved in toluene (15 mL). The resulting solution was refluxed until

most of the free base had coordinated to the metal ion. Upon cooling the reaction mixture to room temperature, dry NaL_{OMe} (0.1 g, 0.22 mmol) was added and the mixture magnetically stirred for another 12 h. After the reaction was complete, the solvent was removed under vacuum and the residue dissolved in chloroform, filtered and chromatographed on silica gel using chloroform/petroleum ether (1:1, v/v) as the eluent. The title product was obtained in about 40–86% yield.

[(NCTPP)Yb(L_{OMe})] (6): Yield 138 mg (70%); m.p. > 300 °C (dec.). ^{1}H NMR ($CDCl_3$): δ = 37.99 (s, 1 H, CH), 30.30 (s, 1 H), 29.64 (s, 1 H), 15.43 (s, 2 H), 15.13 (s, 1 H), 14.80 (s, 1 H), 13.77 (s, 1 H), 13.48 (s, 1 H), 10.46 (t, J = 6.4 Hz, 1 H), 10.26 (t, J = 6.4 Hz, 1 H), 9.76 (d, J = 25.2 Hz, 2 H), 8.10 (s, 1 H), 7.56 (d, J = 30.4 Hz, 2 H), 7.32 (m, 2 H), 7.23–7.18 (m, 2 H), 5.63 (d, J = 40.8 Hz, 18 H), 5.41 (s, 1 H), 5.17 (s, 1 H), 4.17 (s, 1 H), 3.91 (s, 1 H), –1.58 (s, 1 H), –2.45 (s, 1 H), –2.89 (s, 5 H), –5.48 (s, 1 H), –6.20 (s, 1 H) ppm. ^{31}P NMR ($CDCl_3$): δ = 82.8 ppm. $C_{55}H_{51}CoN_4O_9P_3Yb$ (1237.2): calcd. C 53.41, H 4.16, N 4.53; found C 53.28, H 4.33, N 4.36. ESI-HRMS (positive mode in methanol): m/z 1238.1591 $[M + 1]^+$; $C_{55}H_{52}CoN_4O_9P_3Yb$ requires 1238.1678. IR (KBr): $\tilde{\nu}$ = 3428, 2923, 2852, 2360, 2339, 1652, 1594, 1129, 1071, 1037, 1004, 987, 778, 727, 699, 587 cm^{-1}.

[(NCTTP)Yb(L_{OMe})] (7): Yield 103 mg (50%); m.p. > 300 °C (dec.). ^{31}P NMR ($CDCl_3$): δ = 78.1 ppm. $C_{59}H_{59}CoN_4O_9P_3Yb$ (1293.2): calcd. C 54.80, H 4.60, N 4.33; found C 54.68, H 4.63, N 4.36. ESI-HRMS (positive mode in methanol): m/z 1294.2347 $[M + 1]^+$; $C_{59}H_{60}CoN_4O_9P_3Yb$ requires 1294.2293. IR (KBr): $\tilde{\nu}$ = 3425, 2941, 2839, 1599, 1509, 1222, 1135, 1033, 1006, 837, 797, 779, 727, 591 cm^{-1}.

[(NCTFPP)Yb(L_{OMe})] (8): Yield 157 mg (75%); m.p. > 300 °C (dec.). ^{1}H NMR ($CDCl_3$): δ = 37.74 (s, 1 H, CH), 30.16 (s, 1 H), 29.67 (s, 1 H), 15.45 (s, 1 H), 15.32 (s, 1 H), 14.80 (s, 1 H), 14.49 (s, 1 H), 13.75 (s, 1 H), 13.42 (s, 1 H), 9.49–9.56 (m, 2 H), 8.19 (s, 2 H), 7.34–7.46 (m, 3 H), 5.24–5.62 (m, 20 H), 3.97 (s, 1 H), 3.70 (s, 1 H), –1.49 (s, 1 H), –2.10 (s, 1 H), –2.95 (s, 5 H), –5.47 (s, 1 H), –6.21 (s, 1 H) ppm. ^{31}P NMR ($CDCl_3$): δ = 78.0 ppm. $C_{55}H_{47}CoF_4N_4O_9P_3Yb$ (1309.12): calcd. C 50.47, H 3.62, N 4.28; found C 50.98, H 3.63, N 4.26. ESI-HRMS (positive mode in methanol): m/z 1310.1306 $[M + 1]^+$; $C_{55}H_{48}CoF_4N_4O_9P_3Yb$ requires 1310.1301. IR (KBr): $\tilde{\nu}$ = 2940, 2834, 1599, 1505, 1222, 1135, 1090, 1031, 1005, 847, 803, 777, 729, 592 cm^{-1}.

[(NCTCPP)Yb(L_{OMe})] (9): Yield 154 mg (72%); m.p. > 300 °C (dec.). ^{1}H NMR ($CDCl_3$): δ = 37.41 (s, 1 H, CH), 29.98 (s, 1 H), 29.64 (s, 1 H), 15.75 (s, 1 H), 15.33 (s, 2 H), 15.06 (s, 1 H), 13.13 (s, 1 H), 12.72 (s, 1 H), 10.12 (d, J = 41.6 Hz, 2 H), 8.25–7.69 (m, 6 H), 5.96 (s, 1 H), 5.71 (s, 1 H), 5.41 (m, 18 H), 4.53 (s, 1 H), 4.23 (s, 1 H), –1.23 (s, 1 H), –2.05 (s, 1 H), –2.89 (s, 5 H), –5.31 (s, 1 H), –6.08 (s, 1 H) ppm. ^{31}P NMR ($CDCl_3$): δ = 82.0 ppm. $C_{59}H_{47}CoN_8O_9P_3Yb$ (1337.1): calcd. C 53.00, H 3.54, N 8.38; found C 52.98, H 3.57, N 8.36. ESI-HRMS (positive mode in methanol): m/z 1338.1558 $[M + 1]^+$; $C_{59}H_{48}CoN_8O_9P_3Yb$ requires 1338.1488. IR (KBr): $\tilde{\nu}$ = 3401, 2942, 2838, 2225, 1600, 1510, 1475, 1399, 1129, 1037, 1005, 843, 809, 795, 732, 590, 543 cm^{-1}.

[(NCTTEPP)Yb(L_{OMe})] (10): Yield 160 mg (62%); m.p. > 300 °C (dec.). ^{31}P NMR ($CDCl_3$): δ = 79.1 ppm. $C_{75}H_{83}CoN_4O_9P_3Si_4Yb$ (1621.3): calcd. C 55.55, H 5.16, N 3.45; found C 55.76, H 5.17, N 3.50. ESI-HRMS (positive mode in methanol): m/z 1622.3249 $[M + 1]^+$; $C_{75}H_{84}CoN_4O_9P_3Si_4Yb$ requires 1622.3249. IR (KBr): $\tilde{\nu}$ = 3428, 2957, 2850, 2156, 1600, 1499, 1249, 1132, 1037, 1010, 865, 845, 798 cm^{-1}.

[(NCP)Er(L_{OMe})]: The synthesis of Er^{III} complexes followed the same procedures as for Yb^{III} except that solution **B** (2.5 mL, 0.52 mmol Er) was used instead and the clear layer was transferred into a Schlenk flask containing dry NCP (0.16 mmol) in toluene. NaL_{OMe} (0.1 g, 0.22 mmol) was added after refluxing for 12 h. The complex was isolated with a yield of about 50–80% after purification.

[(NCTPP)Er(L_{OMe})] (11): Yield 98 mg (50%); m.p. > 300 °C (dec.). ^{31}P NMR ($CDCl_3$): δ = –123.2 ppm. $C_{55}H_{51}CoErN_4O_9P_3$ (1229.2): calcd. C 53.65, H 4.18, N 4.55; found C 53.45, H 4.29, N 4.38. ESI-HRMS (positive mode in methanol): m/z 1232.1593 $[M + 1]^+$; $C_{55}H_{52}CoErN_4O_9P_3$ requires 1232.1618. IR (KBr): $\tilde{\nu}$ = 2940, 2834, 1594, 1131, 1072, 1032, 1004, 796, 778, 728, 588 cm^{-1}.

[(NCTTP)Er(L_{OMe})] (12): Yield 82 mg (40%); m.p. > 300 °C (dec.). ^{31}P NMR ($CDCl_3$): δ = –128.2 ppm. $C_{59}H_{59}CoErN_4O_9P_3$ (1285.2): calcd. C 55.05, H 4.62, N 4.35; found C 54.98, H 4.63, N 4.32. ESI-HRMS (positive mode in methanol): m/z 1288.2217 $[M + 1]^+$; $C_{59}H_{60}CoErN_4O_9P_3$ requires 1288.2244. IR (KBr): $\tilde{\nu}$ = 3430, 2942, 2918, 2860, 1603, 1509, 1457, 1205, 1182, 1135, 1006, 797, 726, 592 cm^{-1}.

[(NCTFPP)Er(L_{OMe})] (13): Yield 162 mg (78%); m.p. > 300 °C (dec.). ^{31}P NMR ($CDCl_3$): δ = –125.5 ppm. $C_{55}H_{47}CoErF_4N_4O_9P_3$ (1301.1): calcd. C 50.69, H 3.64, N 4.30; found C 50.70, H 3.59, N 4.38. ESI-HRMS (positive mode in methanol): m/z 1304.1241 $[M + 1]^+$; $C_{55}H_{48}CoErF_4N_4O_9P_3$ requires 1304.1232. IR (KBr): $\tilde{\nu}$ = 3422, 2941, 2834, 2225, 1599, 1500, 1473, 1399, 1128, 1036, 1005, 843, 808, 779, 732, 589 cm^{-1}. IR (KBr): $\tilde{\nu}$ = 2941, 2834, 1599, 1505, 1222, 1135, 1090, 1031, 1006, 847, 803, 777, 729, 592 cm^{-1}.

[(NCTCPP)Er(L_{OMe})] (14): Yield 151 mg (71%); m.p. > 300 °C (dec.). ^{31}P NMR ($CDCl_3$): δ = –123.2 ppm. $C_{59}H_{47}CoErN_8O_9P_3$ (1329.1): calcd. C 53.23, H 3.56, N 8.42; found C 53.05, H 3.59, N 8.38. ESI-HRMS (positive mode in methanol): m/z 1332.1448 $[M + 1]^+$, $C_{59}H_{48}CoErN_8O_9P_3$ requires 1332.1428. IR (KBr): $\tilde{\nu}$ = 3422, 2941, 2834, 2225, 1599, 1500, 1473, 1399, 1128, 1036, 1005, 843, 808, 779, 732, 589 cm^{-1}.

[(NCTTEPP)Er(L_{OMe})] (15): Yield 160 mg (70%); m.p. > 300 °C (dec.). ^{31}P NMR ($CDCl_3$): δ = –128.2 ppm. $C_{75}H_{83}CoErN_4O_9P_3Si_4$ (1613.3): calcd. C 55.74, H 5.18, N 3.47; found C 55.66, H 5.17, N 3.50. ESI-HRMS (positive mode in methanol): m/z 1616.3092 $[M + 1]^+$, $C_{75}H_{84}CoN_4O_9P_3Si_4Er$ requires 1616.3196. IR (KBr): $\tilde{\nu}$ = 3435, 2954, 2897, 2834, 2153, 1601, 1499, 1486, 1472, 1249, 1222, 1178, 1129, 1090, 1036, 1008, 864, 844, 760, 730, 658, 588 cm^{-1}.

Preparation of *N*-Methylated Lanthanide *N*-Confused Porphyrinate Complexes [(*N*-CH_3-NCP)Ln(L_{OMe})]$^+$·I^-: [(NCP)Ln(L_{OMe})] (0.7 mmol) was dissolved in CH_2Cl_2 (20 mL) in a flame-dried, 50-mL, two-necked, round-bottomed flask under nitrogen and Cs_2CO_3 (684 mg, 2.1 mmol) and CH_3I (0.31 mL, 2.8 mmol) were added. The reaction mixture was stirred at room temperature for 2 h. After careful TLC monitoring had shown that no [(NCP)Ln(L_{OMe})] was left, the solid was filtered off. Following removal of the solvent, the residue was purified by flash chromatography on a neutral alumina gel column (activity III). Decomposition impurities and a small amount of unreacted [(NCP)Ln(L_{OMe})] were eluted with a solvent mixture of benzene and hexane (80:20, v/v), and the product was eluted with benzene/CH_2Cl_2 (95/5, v/v). The pure product fractions were collected with the spot TLC plates and solvent was removed to give [(*N*-CH_3-NCP)Ln(L_{OMe})]·(I^-) in 96% yield.

[(*N*-CH_3-NCTCPP)Yb(L_{OMe})]$^+I^-$ (16): M.p. > 300 °C (dec.). ^{1}H NMR ($CDCl_3$): δ = 41.64 (s, 1 H, CH), 35.43 (s, 1 H), 32.64 (s, 1 H), 19.24 (s, 1 H), 17.56 (s, 2 H), 16.52 (s, 3 H, CH_3), 16.35 (s, 1 H), 13.85 (s, 1 H), 13.51 (s, 1 H), 11.55 (br., 2 H), 9.77 (s, 1 H), 8.72 (br., 2 H), 8.31 (s, 1 H), 6.32 (br., 1 H), 5.23 (d, J = 5.2 Hz,

Table 3. Crystallographic data for compounds **8**, **9**, **13** and **16**.

Compound	**8**·(2H$_2$O)	**9**·(H$_2$O)	**13**·(2H$_2$O)	**16**
Empirical formula	$C_{55}H_{51}CoF_4N_4O_{11}P_3Yb$	$C_{59}H_{49}CoN_8O_{10}P_3Yb$	$C_{55}H_{51}CoErF_4N_4O_{11}P_3$	$C_{60}H_{50}CoIN_8O_9P_3Yb$
Molecular weight	1344.92	1354.94	1339.10	1478.86
Crystal size [mm]	0.30 × 0.21 × 0.18	0.28 × 0.19 × 0.17	0.30 × 0.24 × 0.22	0.24 × 0.15 × 0.13
Crystal system	monoclinic	monoclinic	monoclinic	triclinic
Space group	$P2_1/n$	$C2/c$	$P2_1/n$	$P\bar{1}$
a [Å]	14.459(2)	30.147(2)	14.4126(7)	14.748(4)
b [Å]	28.423(4)	18.0448(13)	27.4256(13)	15.396(4)
c [Å]	14.721(2)	25.3367(19)	14.8623(7)	16.063(4)
α [°]	90	90	90	75.570(5)
β [°]	113.859(2)	122.8360(10)	114.8750(10)	65.938(4)
γ [°]	90	90	90	64.323(4)
V [Å^3]	5531.2(13)	11580.7(15)	5329.7(4)	2989.8(14)
Z	4	8	4	2
$D_{calcd.}$ [g cm^3]	1.610	1.445	1.646	1.643
T [K]	293	293	293	293
μ(Mo-K_α) [mm^{-1}]	2.144	2.030	2.042	2.491
F(000)	2684	5448	2692	1466
θ range [°]	1.67 to 25.00	1.91 to 25.00	1.81 to 25.00	1.74 to 25.00
Reflections collected	26261	27146	26206	14731
Independent reflections	9601	10097	9363	10289
R_{int}	0.0420	0.0559	0.0253	0.0280
Observed reflections [$I > 2.0\sigma(I)$]	8106	5965	8005	7733
GOF on F^2	1.147	1.083	1.034	1.051
$R1$, $wR2$ [$I > \sigma(I)$][a]	0.0880, 0.2056	0.0659, 0.1628	0.0487, 0.1490	0.0616, 0.1493
$R1$, $wR2$ (all data)	0.1014, 0.2140	0.1354, 0.2172	0.0571, 0.1585	0.0908, 0.1674

[a] $R1 = \Sigma||F_o| - |F_c||/\Sigma|F_o|$; $wR_2 = [\Sigma w(|F_o^2| - |F_c^2|)^2/\Sigma w|F_o^2|^2]^{1/2}$.

18 H), 4.00 (s, 2 H), –2.60 (s, 5 H), –4.86 (s, 1 H), –5.57 (s, 1 H), –7.67 (br., 1 H), –8.00 (s, 1 H) ppm. $^{31}P\{^1H\}$ NMR ($CDCl_3$): δ = 83.2 ppm. ESI-HRMS (positive mode in methanol): m/z 1352.1680 [M – I]$^+$; $C_{60}H_{50}CoN_8O_9P_3Yb$ requires 1352.1639. IR (KBr): $\tilde{\nu}$ = 3401, 2942, 2838, 2227, 1600, 1510, 1475, 1399, 1129, 1037, 1005, 843, 809, 795, 732, 590, 543 cm^{-1}.

[(*N*-CH$_3$-NCTPP)Yb(L$_{OMe}$)]$^+$I$^-$ (17): M.p. > 300 °C (dec.); $^{31}P\{^1H\}$ NMR ($CDCl_3$): δ = 83.2 ppm. ESI-HRMS (positive mode in methanol): m/z 1252.1859 [M – I]$^+$; $[C_{56}H_{54}CoN_4O_9P_3Yb]^+$ requires 1252.1839. IR (KBr): $\tilde{\nu}$ = 3401, 2942, 2838, 1600, 1510, 1475, 1399, 1129, 1037, 1005, 843, 809, 795, 732, 590, 543 cm^{-1}.

[(*N*-CH$_3$-NCTFPP)Er(L$_{OMe}$)]$^+$I$^-$ (18): M.p. > 300 °C (dec.). $^{31}P\{^1H\}$ NMR ($CDCl_3$): δ = –123.2 ppm. ESI-HRMS (positive mode in methanol): m/z 1318.0285 [M – I]$^+$; $[C_{56}H_{50}CoErF_4N_4O_9P_3]^+$ requires 1318.1397. IR (KBr): $\tilde{\nu}$ = 3402, 2942, 2838, 1600, 1510, 1475, 1399, 1129, 1037, 1005, 843, 809, 795, 732, 590, 543 cm^{-1}.

X-ray Crystallography: Single crystals of lanthanide NCP complexes suitable for structural determination were grown by slow evaporation of a methanol solution of the respective complex in air. X-ray intensity data were collected at 293 K on a Bruker Axs SMART 1000 CCD area-detector diffractometer using graphite-monochromated Mo-K_α radiation (λ = 0.71073 Å). The collected frames were processed with the software SAINT[31] and an absorption correction was applied to the collected reflections with SADABS.[32] The structures were solved by direct methods and expanded by standard difference Fourier syntheses using the software SHELXTL.[33] Structure refinements were made on F^2 using the full-matrix least-squares technique. All non-hydrogen atoms were refined with anisotropic displacement parameters. Hydrogen atoms were placed in their idealized positions and allowed to ride on the respective carbon atoms. Pertinent crystallographic data and other experimental details are summarized in Table 3.

CCDC-673159 (for **8**), -673160 (for **9**), -673161 (for **13**), and -673162 (for **16**) contain the supplementary crystallographic data for this paper. These data can be obtained free of charge from The Cambridge Crystallographic Data Center via www.ccdc.cam.ac.uk/data_request/cif.

Acknowledgments

We thank the Hong Kong Baptist University (FRG/05-06/I-12 and FRG/05-06/II-03) and the Hong Kong Research Grants Council (HKBU 2021/03P) for their financial support.

[1] H. Furuta, T. Asano, T. Ogawa, *J. Am. Chem. Soc.* **1994**, *116*, 767–768.
[2] P. J. Chmielewski, L. Latos-Grażyński, K. Rachlewicz, T. Glowiak, *Angew. Chem. Int. Ed. Engl.* **1994**, *33*, 779–781.
[3] J. L. Sessler, *Angew. Chem. Int. Ed. Engl.* **1994**, *33*, 1348–1350.
[4] L. Latos-Grażyński, in *The Porphyrin Handbook* (Eds.: K. M. Kadish, K. M. Smith, R. Guilard), Academic Press, San Diego, **1999**, vol. 2, chapter 14.
[5] G. R. Geier III, D. M. Haynes, J. S. Lindsey, *Org. Lett.* **1999**, *1*, 1455–1458.
[6] H. Furuta, T. Ishizuka, A. Osuka, H. Dejima, H. Nakagawa, Y. Ishikawa, *J. Am. Chem. Soc.* **2001**, *123*, 6207–6208.
[7] a) H. Furuta, H. Maeda, A. Osuka, *J. Am. Chem. Soc.* **2000**, *122*, 803–807; b) A. Srinivasan, H. Furuta, *Acc. Chem. Res.* **2005**, *38*, 10–20; c) H. Maeda, H. Furuta, *Pure Appl. Chem.* **2006**, *78*, 29–44; d) M. G. P. M. S. Neves, R. M. Martins, A. C. Tomé, A. J. D. Silvestre, A. M. S. Silva, V. Félix, M. G. B. Drew, J. A. S. Cavaleiro, *Chem. Commun.* **1999**, 385–386; e) A. Srinivasan, T. Ishizuka, A. Osuka, H. Furuta, *J. Am. Chem. Soc.* **2003**, *125*, 878–879.
[8] a) P. J. Chmielewski, L. Latos-Grazynski, *Coord. Chem. Rev.* **2005**, *249*, 2510–2533; b) J. D. Harvey, C. J. Ziegler, *Coord. Chem. Rev.* **2003**, *247*, 1–19; c) H. Furuta, H. Maeda, A.

Osuka, *Chem. Commun.* **2002**, 1795–1804; d) J. D. Harvey, C. J. Ziegler, *J. Inorg. Biochem.* **2006**, *100*, 869–880; e) T. D. Lash, *Eur. J. Org. Chem.* **2007**, 5461–5481; f) D. Wu, A. B. Descalzo, F. Weik, F. Emmerling, Z. Shen, X.-Z. You, K. Rurack, *Angew. Chem. Int. Ed.* **2008**, *47*, 193–197; g) R. Misra, R. Kumar, T. K. Chandrashekar, B. S. Joshi, *J. Org. Chem.* **2007**, *72*, 1153–1160.

[9] a) W.-C. Chen, C.-H. Hung, *Inorg. Chem.* **2001**, *40*, 5070–5071; b) D. S. Bohle, W.-C. Chen, C.-H. Hung, *Inorg. Chem.* **2002**, *41*, 3334–3336; c) K. Rachlewicz, S. L. Wang, C.-H. Peng, C.-H. Hung, L. Latos-Grażyński, *Inorg. Chem.* **2003**, *42*, 7348–7350.

[10] a) H. Furuta, T. Ogawa, Y. Uwatoko, K. Araki, *Inorg. Chem.* **1999**, *38*, 2676–2682; b) H. Maeda, A. Osuka, Y. Ishikawa, I. Aritome, Y. Hisaewa, H. Furuta, *Org. Lett.* **2003**, *5*, 1293–1296; c) H. Maeda, Y. Ishikawa, T. Matsuda, A. Osuka, H. Furuta, *J. Am. Chem. Soc.* **2003**, *125*, 11822–11823; d) H. Maeda, A. Osuka, H. Furuta, *J. Am. Chem. Soc.* **2003**, *125*, 15690–15691; e) S. Mori, A. Osuka, *J. Am. Chem. Soc.* **2005**, *127*, 8030–8031; f) S. Mori, K. S. Kim, Z. S. Yoon, S. B. Noh, D. Kim, A. Osuka, *J. Am. Chem. Soc.* **2007**, *129*, 11344–11345.

[11] a) P. J. Chmielewski, L. Latos-Grażyński, T. Glowiak, *J. Am. Chem. Soc.* **1996**, *118*, 5690–5701; b) H. Furuta, N. Kubo, H. Maeda, Y. Ishikawa, A. Osuka, H. Nanami, T. Ogawa, *Inorg. Chem.* **2000**, *39*, 5424–5425; c) P. J. Chmielewski, L. Latos-Grażyński, I. Schmidt, *Inorg. Chem.* **2000**, *39*, 5475–5482; d) C.-H. Hung, W.-C. Chen, G.-H. Lee, S.-M. Peng, *Chem. Commun.* **2002**, 1516–1517; e) H. Furuta, K. Youfu, H. Maeda, A. Osuka, *Angew. Chem. Int. Ed.* **2003**, *42*, 2186–2188; f) K. Rachlewicz, S.-L. Wang, J.-L. Ko, C.-H. Hung, L. Latos-Grażyński, T. Glowiak, *J. Am. Chem. Soc.* **2004**, *126*, 4420–4431.

[12] a) H. Furuta, T. Ishizuka, A. Osuka, *J. Am. Chem. Soc.* **2002**, *124*, 5622–5623; b) H. Furuta, T. Morimoto, A. Osuka, *Inorg. Chem.* **2004**, *43*, 1618–1624; c) M. Toganoh, T. Niino, H. Maeda, B. Andrioletti, H. Furuta, *Inorg. Chem.* **2006**, *45*, 10428–10430.

[13] a) W.-K. Wong, L.-L. Zhang, W.-T. Wong, F. Xue, T. C.-W. Mak, *J. Chem. Soc., Dalton Trans.* **1999**, 615–622; b) J.-X. Meng, K.-F. Li, J. Yuan, L.-L. Zhang, W.-K. Wong, K.-W. Cheah, *Chem. Phys. Lett.* **2000**, *332*, 313–318; c) W.-K. Wong, A.-X. Hou, J.-P. Guo, H.-S. He, L.-L. Zhang, W.-Y. Wong, K.-F. Li, K.-W. Cheah, F. Xue, T. C.-W. Mak, *J. Chem. Soc., Dalton Trans.* **2001**, 3092–3098; d) W.-K. Wong, X.-J. Zhu, W.-Y. Wong, *Coord. Chem. Rev.* **2007**, *251*, 2386–2399.

[14] T. J. Foley, B. S. Ha, S. Knefely, K. A. Abboud, J. R. Reynolds, K. S. Schanze, J. M. Boncella, *Inorg. Chem.* **2003**, *42*, 5023–5032.

[15] X.-J. Zhu, W.-K. Wong, W.-K. Lo, W.-Y. Wong, *Chem. Commun.* **2005**, 1022–1024.

[16] a) P. Rothemund, *J. Am. Chem. Soc.* **1939**, *61*, 2912–2915; b) P. Rothemund, A. R. Menotti, *J. Am. Chem. Soc.* **1941**, *63*, 267–270; c) A. D. Alder, F. R. Longo, J. D. Finarelli, J. Goldmacher, J. Assour, L. Korsakoff, *J. Org. Chem.* **1967**, *32*, 476–476.

[17] G. R. Geier III, J. S. Lindsey, *J. Org. Chem.* **1999**, *64*, 1596–1603.

[18] S. J. Narayanan, B. Sridevi, A. Srinivasan, T. K. Chandrashekar, R. Roy, *Tetrahedron Lett.* **1998**, *39*, 7389–7392.

[19] a) J. P. Belair, C. J. Ziegler, C. S. Rajesh, D. A. Modarelli, *J. Phys. Chem. A* **2002**, *106*, 6445–6451; b) E. A. Alemán, C. S. Rajesh, C. J. Ziegler, D. A. Modarelli, *J. Phys. Chem. A* **2006**, *110*, 8605–8612; c) J. L. Shaw, S. A. Garrison, E. A. Alemán, C. J. Ziegler, D. A. Modarelli, *J. Org. Chem.* **2004**, *69*, 7423–7427.

[20] a) R. S. Macomber, *A Complete Introduction to Modern NMR Spectroscopy*, Wiley-Interscience, New York, **1988**, p. 168; b) J. A. Peters, J. Huskens, D. J. Raber, *Prog. Nucl. Magn. Reson. Spectrosc.* **1996**, *28*, 283–350.

[21] C. Platas, F. Avecilla, A. de Blas, C. F. G. C. Geraldes, T. Rodríguez-Blas, H. Adams, J. Mahía, *Inorg. Chem.* **1999**, *38*, 3190–3199.

[22] W. R. Gerd, D. B. Christian, P. A. Y. Glenn, *Inorg. Chem.* **2001**, *40*, 4780–4784.

[23] M. P. Oude Wolbers, F. C. J. M. van Veggel, B. H. M. Snellink-Ruel, J. W. Hofstraat, F. A. J. Geuets, D. N. Reinhoudt, *J. Chem. Soc. Perkin Trans. 2* **1998**, 2141–2150.

[24] M. H. V. Werts, J. W. Verhoeven, J. W. Hofstaat, *J. Chem. Soc. Perkin Trans. 2* **2000**, 433–439.

[25] a) W. D. Horrocks Jr, J. P. Bolender, W. D. Smith, R. M. Supkowski, *J. Am. Chem. Soc.* **1997**, *119*, 5972–5973; b) F. J. Steemers, W. Verboom, J. W. Hofstraat, F. A. J. Geurts, D. N. Reinhoudt, *Tetrahedron Lett.* **1998**, *39*, 7583–7586; c) L. H. Slooff, A. Polman, A. I. Klink, G. A. Hebbink, L. Grave, F. C. J. M. van Veggel, D. N. Reinhoudt, J. W. Hofstraat, *Opt. Mater.* **2000**, *14*, 101–107; d) M. H. V. Werts, R. H. Woudennberg, P. G. Emmerink, R. van Gassel, J. W. Hofstraat, J. W. Verhoeven, *Angew. Chem. Int. Ed.* **2000**, *39*, 4542–4544; e) S. I. Klink, G. A. Hebbink, L. Grave, F. G. Peters, F. C. J. M. Van Veggel, D. N. Reinhoudt, J. W. Hofstraat, *Eur. J. Org. Chem.* **2000**, *2000*, 1923–1931; f) F. Vögtle, M. Gorka, V. Vicinelli, P. Ceroni, M. Maestri, V. Balzani, *ChemPhysChem* **2001**, *2*, 769–773; g) F. R. Goncalvese Silva, O. L. Malta, C. Reinhard, H. Güdel, C. Piguet, J. E. Moser, J. G. Bünzli, *J. Phys. Chem. A* **2002**, *106*, 1670–1677; h) S. I. Klink, H. Keizer, H. W. Hofstraat, F. C. J. M. van Veggel, *Synth. Met.* **2002**, *127*, 213–216; i) G. A. Hebbink, S. I. Klink, L. Grave, P. G. B. Oude Alink, F. C. J. M. van Veggel, *ChemPhysChem* **2002**, *3*, 1014–1018; j) P. B. Glover, P. R. Ashton, L. J. Childs, A. Rodger, M. Kercher, R. M. Williams, L. De Cola, Z. Pikramenou, *J. Am. Chem. Soc.* **2003**, *125*, 9918–9919; k) S. Faulkner, S. J. A. Pope, *J. Am. Chem. Soc.* **2003**, *125*, 10526–10527; l) N. M. Shavaleev, L. P. Moorcraft, S. J. A. Pope, Z. R. Bell, S. Faulkner, M. D. Ward, *Chem. Eur. J.* **2003**, *9*, 5283–5291; m) G. A. Hebbink, L. Grave, L. A. Woldering, D. N. Reinhout, F. C. J. M. van Veggel, *J. Phys. Chem. A* **2003**, *107*, 2483–2491; n) D. Imbert, M. Cantue, J.-C. G. Bunzli, G. Bernardinelli, C. Piguet, *J. Am. Chem. Soc.* **2003**, *125*, 15698–15699; o) G. M. Davies, R. J. Aarons, G. R. Motson, J. C. Feffery, H. Adams, S. Faulkner, M. D. Ward, *Dalton Trans.* **2004**, 1136–1144; p) J.-C. G. Bünzli, C. Piguet, *Chem. Soc. Rev.* **2005**, *34*, 1048–1077; q) M. D. Ward, *Coord. Chem. Rev.* **2007**, *251*, 1663–1677; r) T. Lazarides, G. M. Davies, H. Adams, C. Sabatini, F. Barigelletti, A. Barbieri, S. J. A. Pope, S. Faulkner, M. D. Ward, *Photochem. Photobiol. Sci.* **2007**, 1152–1157; s) S. G. Baca, H. Adams, D. Sykes, S. Faulkner, M. D. Ward, *Dalton Trans.* **2007**, 2419–2430.

[26] a) H. He, J. Guo, Z. Zhao, W.-K. Wong, W.-Y. Wong, W.-K. Lo, K.-F. Li, K.-W. Cheah, *Eur. J. Inorg. Chem.* **2004**, 837–845; b) H. He, W.-K. Wong, K.-F. Li, K.-W. Cheah, *Synth. Met.* **2004**, *143*, 81–87.

[27] H. S. He, Z.-X. Zhao, W.-K. Wong, K.-F. Li, J.-X. Meng, K.-W. Cheah, *Dalton Trans.* **2003**, 980–986.

[28] a) K. Kalyanasundaram, *Photochemistry of Polypyridine and Porphyrin Complexes*, Academic Press, London, **1992**, p. 376; b) K. Kalyanasundaram, *Photochemistry of Polypyridine and Porphyrin Complexes*, Academic Press, London, **1992**, p. 409.

[29] G. A. Hebbink, D. N. Reinhoudt, F. C. J. M. van Veggel, *Eur. J. Org. Chem.* **2001**, *21*, 4101–4106 and references cited therein.

[30] C. A. Parker, W. T. Rees, *Analyst (London)* **1960**, *85*, 587–600.

[31] *SAINT*+, ver. 6.02a, Bruker Analytical X-ray System, Inc., Madison, WI, **1998**.

[32] G. M. Sheldrick, *SADABS*, Empirical Absorption Correction Program; University of Göttingen, Germany, **1997**.

[33] G. M. Sheldrick, *SHELXTL*^{TM}, Reference manual, version 5.1, Madison, WI, **1997**.

Received: March 13, 2008
Published Online: June 10, 2008

